Net-Baryon Physics: Basic Mechanisms

J. Alvarez-Muñiz[1], R. Conceição[a,3], J. Dias de Deus[2,4], M.C. Espírito Santo[2,3], J. G. Milhano[2,4], M. Pimenta[2,3]

***Abstract*— How does the fraction of energy carried by the net-baryon, $B - \bar{B}$, evolve as a function of the centre-of-mass collisional energy per nucleon, $\sqrt{s}$? In order to answer this question we explore the net-baryon mechanism and it is propose a simple but consistent model for net-baryon production in high energy hadron-hadron, hadron-nucleus and nucleus-nucleus collisions. The model basic ingredients are: valence string formation based on standard PDFs with QCD evolution; and string fragmentation via the Schwinger mechanism. Our model shows that a good description of the main features of net-baryon data is possible in the framework of a simplistic model, with the advantage of making the fundamental production mechanisms manifest. We compare results both with data and existing models.**

I. Introduction

An important question to be asked is: how does the fraction of energy carried by the net-baryon, $B - \bar{B}$, evolve as a function of the centre-of-mass collisional energy per nucleon, $\sqrt{s}$? Net-baryon keeps track of the energy-momentum carried by the incoming particles thus there are two reasons why it is important to answer this question: the first one is that a decrease of the fraction of energy going the net-baryon implies more energy available to create the deconfined quark-gluon state of matter, and the second one is that such a decrease may reduce the possibility of producing fast particles in very high energy cosmic ray experiments.

For more than 30 years, since the ISR at CERN, particle production studies have been limited to mid rapidity. Fortunately, with RHIC, large rapidity data became available, and, hopefully, the same will happen for the LHC. In fact, if one does not measure the physics at high rapidity the most elementary physical constraint, namely energy conservation, cannot be applied [1], [2]. In most of the existing Monte Carlo models [3], [4], [5], [6], the physics of net-baryon production is very much obscured by the complexity of extensive and detailed codes. Often, the basic production mechanisms do not appear in a transparent way.

Based in the Dual Parton Model (DPM) picture, we present a simple model for the production of the net-baryon in hadron-hadron (h-h), hadron-nucleus (h-A) and nucleus-nucleus (A-A) collisions. The basic ingredients of the model are:

- Formation of extended color fields or strings, making use of PDFs for valence quarks;
- Evolution with momentum transfer Q^2, as a consequence of the QCD evolution of the PDF's;
- Fragmentation of each string with formation of a fast baryon (net-baryon) and other particles.

With this simple model we show that a significant part of the physics of net-baryon production can be understood in terms of valence strings and Q^2 evolution, while sea strings play a less relevant role.

II. Review of current model predictions and experimental data

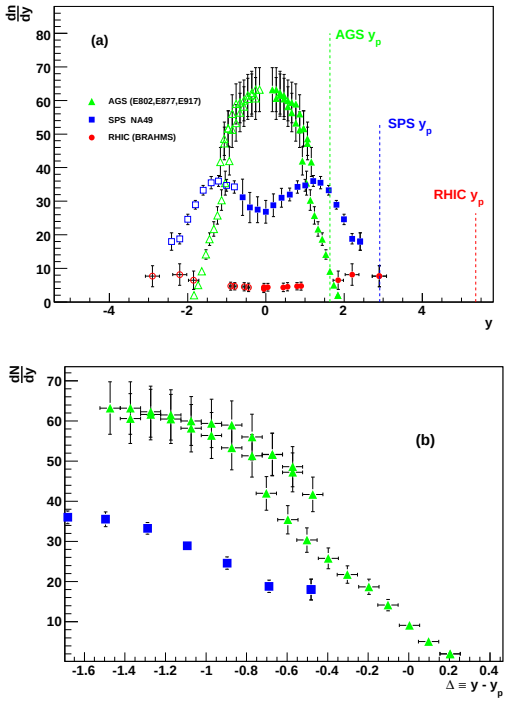

Fig. 1. (a) The net-proton distribution at AGS [12] (Au+Au at $\sqrt{s} \simeq 5$ GeV), SPS [13] (Pb+Pb at $\sqrt{s} \simeq 17$ GeV), and RHIC [10] (Au+Au at $\sqrt{s} = 200$ GeV) is shown. The data correspond to the 5% (4% and 3% for E877 and E802, respectively) most central collisions and the errors are both statistical and systematic. The data have been symmetrised. For RHIC data, filled points are measured and open points are symmetrised, while the opposite is true for AGS and SPS data (for clarity). At AGS weak decay corrections are negligible and at SPS they have been applied. They have been computed and included for RHIC data following [10]. (b) The distribution of $\Delta \equiv y - y_p$ is shown for SPS and AGS data.

The data presently available on net-proton or net-baryon production is scarce. The most recent results are from RHIC [10]. These results are presented both in terms of net-baryon rapidity y and in terms of rapidity loss, defined as

$$\langle \delta y \rangle = y_p - \langle y \rangle \ , \tag{1}$$

[1]IGFAE and Dep. Fisica Particulas, Univ. Santiago de Compostela, 15782 Santiago de Compostela, Spain
[2]Departamento de Física, IST, Av. Rovisco Pais, 1049-001 Lisboa, Portugal
[3]LIP, Av. Elias Garcia, 14-1, 1000-149 Lisboa, Portugal
[4]CENTRA, Av. Rovisco Pais, 1049-001 Lisboa, Portugal
[a]Corresponding author: ruben@lip.pt

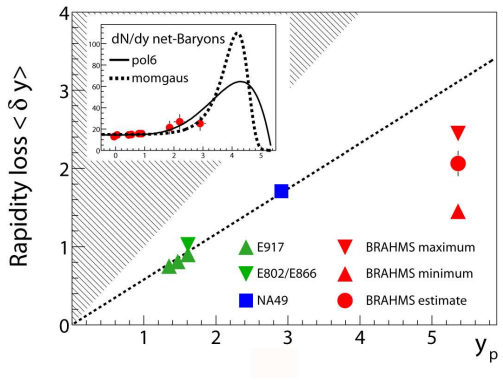

Fig. 2. Rapidity loss as a function of beam rapidity (in the CM). The hatched area indicates the unphysical region, and the dashed line shows the phenomenological scaling $\langle \delta y \rangle = 0.58 y_p$. The inset plot shows the BRAHMS net-baryon distribution (data points) with fits (lines) needed to extrapolate up to the beam rapidity, explaining the large uncertainty associated to the BRAHMS rapidity loss measurement. Taken from [10].

where y_p is the beam rapidity and $\langle y \rangle$ is the mean net-baryon rapidity after the collision, given by

$$\langle y \rangle = \frac{2}{N_{part}} \int_0^{y_p} y \frac{dN_{B-\bar{B}}(y)}{dy} dy \,. \qquad (2)$$

Here, N_{part} is the number of participants in the collision and $N_{B-\bar{B}}$ is the net-baryon number. It is worth noting that the net-baryon results depend directly on the number of participants in the collision and thus on the collision centrality. The relation between the number of participants and the impact parameter of the collision can be established, for instance, in the context of the Glauber model [11].

In figure 1(a), the net-proton distributions at AGS (Au+Au at $\sqrt{s} \simeq 5$ GeV) [12], SPS (Pb+Pb at $\sqrt{s} \simeq 17$ GeV) [13], and RHIC (Au+Au at $\sqrt{s} = 200$ GeV) [10] for central collisions are shown. The 5% most central collisions have been selected, except for E877 and E802 data, which are for the 4% and 3% most central collisions, respectively. The distributions show a strong energy dependence, with the mid rapidity region corresponding to a peak at AGS, a dip at the SPS, and a broad minimum at RHIC. Weak decay corrections (removing the contribution from protons/antiprotons produced not at vertex but from strange baryon decays) are negligible at AGS and have been applied for SPS data. For RHIC data they have been computed and included, following [10] and considering that the RHIC data are concentrated in the mid-rapidity region. From [10], the feed-down correction factor (including both the Λ and the Σ contribution) in the mid-rapidity region can be estimated as 0.65, with an uncertainty below 20%.

The distribution of $\Delta = y - y_p$ computed from the previous plot is shown in figure 1(b) for SPS and AGS data. It is apparent that neither Feynman scaling nor limiting fragmentation are satisfied in net-baryon production.

In figure 2, the rapidity loss data is shown as a function of the beam rapidity (in the centre-of-mass frame) for AGS, SPS and RHIC. The large uncertainty associated with the BRAHMS data point is, as illustrated in the inset plot, related to a relatively unconstrained extrapolation to the high rapidity region, required for the rapidity loss calculation.

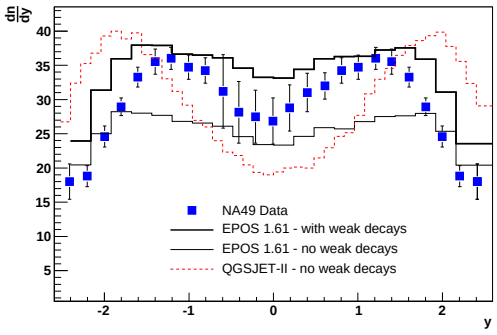

Fig. 3. The net-proton rapidity distributions from EPOS 1.61 (full lines) and QGSJET-II.03 (dashed line) for Pb-Pb collisions at $\sqrt{s} \simeq 17$ GeV are shown and compared with data NA49 SPS data (points) with weak decay corrections [13]. For EPOS, the results obtained including (thick line) and excluding (thin line) the strangeness contribution are shown. For QGSJET, the "no-decays" curve is shown. For details on the data see figure 1

Let us now turn to net-baryon production as implemented in the existing Monte Carlo models. QGSJET-II [4] and EPOS [5] are amongst the presently most widely used hadronic models in high energy and cosmic ray physics. To our knowledge, there is no systematic study comparing the predictions of these two models on net-baryon production between themselves or with experimental data.

In figure 3, net-proton rapidity distributions obtained with QGSJET-II.03 and EPOS 1.61 for Pb-Pb collisions at $\sqrt{s} \simeq 17$ GeV are shown and compared with experimental data. It is possible to see that neither QGSJET-II.03 or EPOS 1.61 can reproduce satisfactorily the net-proton features at this energy. QGSJET-II.03 aims at high energy physics (RHIC and above) and is not expected to perform as well at such low energies.

III. The Model

In this section we will describe our simple model for the net-baryon production. The basic assumption is that the net-baryon producion in proton-proton collisions is strongly correlated with the formation and fragmentation of two color singlet strings [7], [8], [9], [15]. These strings will have two valence quarks from one proton at one end and one valence quark from the other proton at the opposite end of the string, as shown in figure 4.

Referring to the figure, let x_1, x_2 and x_3 be the fractions of momentum carried by the valence quarks forming string A. Quarks 1 and 2 are from the proton with positive momentum in the proton-proton reference frame, and quark 3 is from the other proton. No transverse momentum is considered within this model. By choice, $x_1 > x_2 > x_3$, with $x_3 < 0$. The energy and momentum of each string are obtained adding directly the energy and momentum carried by each of the valence quarks. For string A

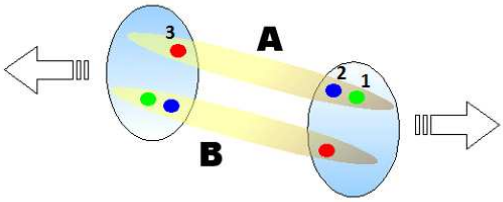

Fig. 4. Schematic representation of a proton-proton collision, with the formation of two valence strings.

$$E_{string} = (x_1 + x_2 + (-x_3))\frac{\sqrt{s}}{2}, \quad (3)$$

$$P_{string} = (x_1 + x_2 - (-x_3))\frac{\sqrt{s}}{2}, \quad (4)$$

$$M_{string} = \sqrt{(x_1 + x_2)\ (-x_3)\ s}, \quad (5)$$

where the quark momentum fractions x_1, x_2 and x_3 are determined from the valence quark PDFs (CTEQ6M [16] in this work) at an effective momentum transfer Q^2. For each $\sqrt{s}$, there is a corresponding effective Q^2 which can be derived from the data.

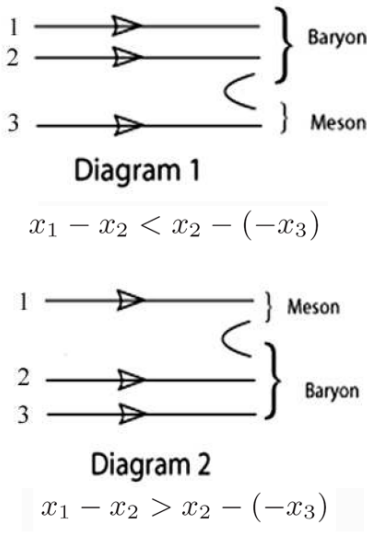

Fig. 5. The two main valence string fragmentation diagrams. In the simple model assumed, the string is cut in two pieces and a $q\bar{q}$ pair is formed, from the vacuum, between the two quarks with the largest momentum difference. Diagram 1 corresponds to the case $x_1 - x_2 < x_2 - (-x_3)$, in which quarks 2 and 3 (belonging to different protons) are chosen. In Diagram 2, $x_1 - x_2 > x_2 - (-x_3)$ and string fragmentation occurs between quarks 1 and 2 (belonging to the same proton).

The hadronization is done by implementing the simplest fragmentation model possible. Each string decays into a baryon and a meson in the following way: the string is cut in two pieces and a $q\bar{q}$ pair is formed, from the vacuum, either between quarks 2 and 3 (belonging to different protons) or between quarks 1 and 2 (belonging to the same proton, with positive momentum in the case of string A). The string is cut between the two quarks with the largest momentum difference. The string piece that inherits two valence quarks originates the baryon, whereas the string piece that inherits one valence quark originates the meson. This mechanism corresponds to the diagrams represented in figure 5. Diagram 1 corresponds to the case $x_1 - x_2 < x_2 - (-x_3)$, in which quarks 2 and 3 are chosen to form a baryon. In Diagram 2, $x_1 - x_2 > x_2 - (-x_3)$ and string fragmentation occurs between quarks 1 and 2. The weights of the two diagrams are, in this simple model, given only by kinematics. For string A the first diagram will be more probable (especially for low $\sqrt{s}$). However, the weight of the second diagram can be as large as 40% above LHC energies.

The $q\bar{q}$ pair formed from the vacuum was taken to be either a $u\bar{u}$ or a $d\bar{d}$, and the full quark combinatorics was then performed in order to determine the nature of the possible outcoming baryon. Both fundamental and excited states were considered, taking spin-dependent weights (2j+1). The decays of the unstable baryons were then performed and the outcoming nucleons included in the net-baryon calculations. The contribution from s quarks was not considered here. It should be noted that the rapidity distribution obtained not including $s\bar{s}$ pairs in the model is well suited for comparing to data with weak decay corrections included. The strangeness effect is in this case simply a global factor. It was estimated from the Schwinger model to be about 25% to 35%.

It is shown in figure 6 the rapidity distributions for different values of Q^2, for proton-proton collisions at two different centre-of-mass energies. It is worth noting that the evolution of the curves varies with Q^2 but also with $\sqrt{s}$, due to kinematic effects in the string fragmentation.

The inclusion of diagram 2, in addition to diagram 1, with weights determined simply by kinematics, reproduces some of the effects predicted in models with string junctions [17], [18] or popcorn [19] mechanisms for the transport of baryon number from the beam rapidity into the central region $y \sim 0$. These effects can thus be achieved in a simple DPM model, based on valence strings and a Q^2 parameterisation, in the spirit of [9], [18], [15].

It is thus apparent that in this simple model $dn/dy(B - \bar{B})$ is obtained from the rapidity of the two baryons produced in the fragmentation of the valence strings. For the purpose of estimating the net-baryon production in A-A collisions, we shall use the simple approximation that $dn/dy(B - \bar{B})$ at a given $\sqrt{s}$ is proportional to the number of participating nucleons, N_{part},

$$\frac{dn}{dy}(B - \bar{B})\Big|_{A-A} \simeq \frac{1}{2} N_{part} \times \frac{dn}{dy}(B - \bar{B})\Big|_{p-p}. \quad (6)$$

This relation is presumably reasonable as net-baryon production is originated from valence strings associated to wounded (or participating) nucleons. An attempt to estimate nuclear effects correction factors for the valence quark PDFs

was made using EKS98 [20] and nDS [21]. Values below 10-15% were found.

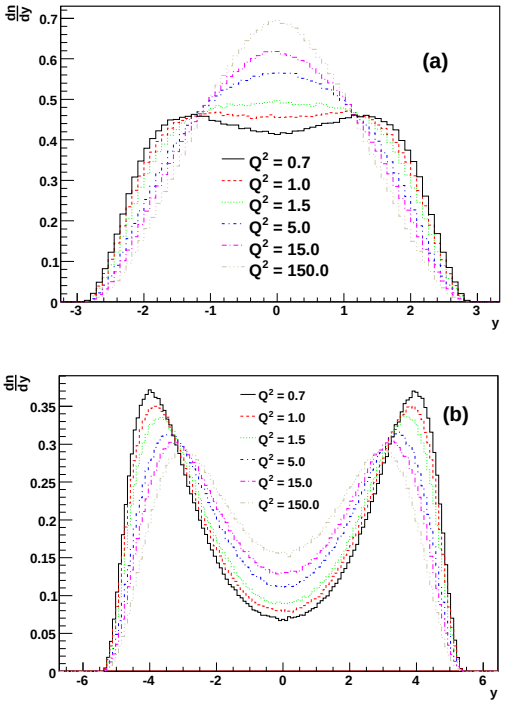

Fig. 6. Evolution of the net-baryon rapidity with Q^2 (in (GeV/c)^2) for proton-proton collisions at (a) $\sqrt{s} = 17$ GeV and (b) $\sqrt{s} = 200$ GeV.

IV. Results

In order to fully define the model, we need to choose an effective Q^2 value as input for the quark PDFs. This is done by adjusting the results of the model to the experimental data, i.e., by choosing, for each $\sqrt{s}$, the effective Q^2 for which the model better describes the data reviewed in section II (see figure 1). Weak decay corrections have been taken into account. In the fitting procedure, the global normalisation factor (the number of participants, relying on the approach of eq. (6)) is left as a second free parameter. In this way we reduce the dependence on the Glauber model, and have also an important crosscheck. In order to compare the results of this model on net-baryon to the experimental data on net-proton, we consider that net-proton is roughly 1/2 of $(B - \bar{B})$ [10].

At $\sqrt{s} = 200$ GeV and $\sqrt{s} \simeq 17$ GeV all the data points (see figure 7) were included in the fit. At $\sqrt{s} \simeq 5$ GeV only the points up to the nominal beam rapidity were considered, since our simple model does not include Fermi momentum effects in the incident nucleus, relevant at such low energies, and therefore has no mechanism to reproduce these data.

Figure 7 shows the results of the present model for net-proton rapidity distribution in comparison with experimental data at different centre-of-mass energies. A good agreement is found at the measured energies. Concerning the 200 GeV case, it should be noted that present RHIC data cover only the mid-rapidity range, leaving the fit largely unconstrained. Although a good fit to the data is obtained, with $Q^2 \simeq 92$ GeV^2, $N_{part} \simeq 113$, the errors are thus extremely large, and we are not able to establish constrained bounds on the parameters of the model. The values obtained for the effective Q^2 and the number of participants N_{part} at $\sqrt{s} \simeq 5$ GeV and $\sqrt{s} \simeq 17$ GeV are given in table I. At these energies, the values obtained for the errors on the fit parameters are reasonably small.

$\sqrt{s}$ (GeV)	Collision	Q^2 (GeV^2)	N_{part}
5	Au-Au	$0.30^{+0.04}_{-0.01}$	$269.9^{+10.4}_{-9.0}$
17	Pb-Pb	$0.77^{+0.18}_{-0.04}$	$299.6^{+9.7}_{-7.7}$

TABLE I

Results of the fit to the effective Q^2 and the number of participants.

It is worth noting that the fitted N_{part} values are close to what is expected from the literature if one takes into account that strangeness contribution was not considered. In fact, the average number of participants for Pb-Pb collisions at SPS energies is given in [14] as 362. As pointed out in section III, the strangeness contribution to the net-baryon amounts to about 25% to 35%, accounting for the value obtained for the number of participants at $\sqrt{s} \simeq 17$ GeV. Concerning Au-Au collisions, the value is expected to be only slightly lower (estimated as 344 to 357 at RHIC energies [10], [22], [23]) and expected to depend weakly on $\sqrt{s}$, in fair agreement with the obtained results. Even though the strangeness contribution should be much smaller, low energy effects are not taken into account in the model and can contribute to the result at $\sqrt{s} \simeq 5$ GeV.

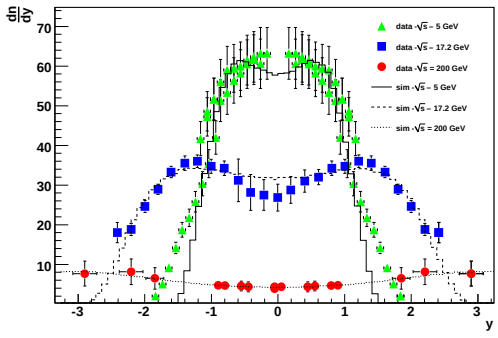

Fig. 7. The results of the present model for net-proton rapidity are compared to experimental data for nucleus-nucleus (A-A) collisions at different centre-of-mass energies. See figure 1 for details on the data points.

We can now try to find a relation between the effective Q^2 and $\sqrt{s}$. The effective Q^2 corresponds to the typical transverse size (area) of the parton (here, the valence quark). It is reasonable to assume, as in Regge phenomenology [24], that the average number of partons in a nucleon increases as a

power of the centre of mass energy $\sqrt{s}$. Thus, $\sqrt{s}/Q^2 \sim R_h^2$, where R_h is the nucleon radius which we take as fixed. It then follows that Q^2 should grow according to

$$Q^2 = Q_0^2 \left(\frac{\sqrt{s}}{\sqrt{s_0}} \right)^{\lambda_v} \left[GeV^2 \right]. \qquad (7)$$

The exponent λ_v was determined by fitting eq. (7) to the available data points in table I.

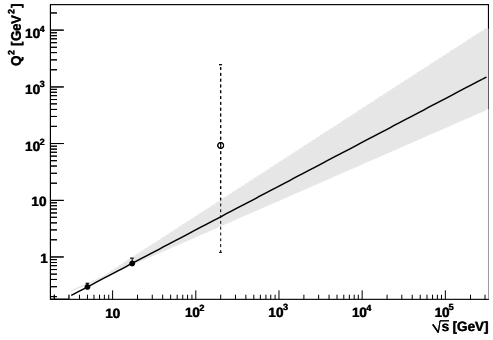

Fig. 8. The effective Q^2 values at different centre-of-mass energies chosen by tuning the model to the experimental data are shown. The line shows the fit to the two lowest energy points using eq. (7). The $\sqrt{s} = 200$ GeV point is shown in dashed only to stress that it does not put any effective constraint on the value of Q^2 (see text). The shaded areas correspond to 1σ variations of the fit parameters.

The results are shown in figure 8, where the data points are the Q^2 values adjusted above, the line is the fit with eq. (7) and the shaded areas correspond to 1σ variations of the fit parameters. Only the data points at $\sqrt{s} \simeq 5$ GeV and $\sqrt{s} \simeq 17$ GeV (given in table I) were included in the fit. The point obtained at $\sqrt{s} = 200$ GeV is shown in dashed only to stress that, as stated above, the error bars are so large that this result does not put any effective constraint on the value of Q^2. The obtained results are $\lambda_v = 0.77^{+0.18}_{-0.13}$ and $Q_0^2 = 0.30^{+0.05}_{-0.01}$, taking $\sqrt{s_0} = 5$ GeV. It should be noted that we have only two points in the fit and the 1σ band is very wide, and thus our estimate of Q^2 at very high energies is very rough. This fact underlines the need for net-baryon data at high energies. However, and as it is apparent already in figure 6(b) at $\sqrt{s} = 200$ GeV, at high Q^2 (and high energies) there is a kind of saturation effect such that the dependence on Q^2 becomes weaker in high rapidity regions. The effects of this large uncertainty are nevertheless taken into account below.

The predictions of the present model for net-baryon rapidity and rapidity loss at higher centre-of-mass energies were then obtained and are shown in figure 9, covering both the LHC and the high energy cosmic ray regions. The width of the curves corresponds to varying the Q^2 within the 1σ band shown in figure 8. In addition, the fraction of the centre-of-mass energy carried by the net-baryon as a function of $\sqrt{s}$ was computed and is shown in figure 10 (together with the 1σ bounds). The

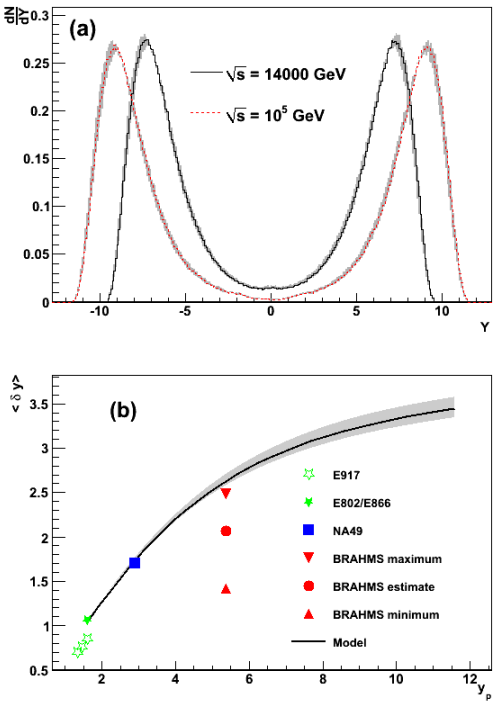

Fig. 9. Predictions of the present model for (a) net-baryon rapidity and (b) rapidity loss in proton-proton collisions at higher energies.

predictions of EPOS 1.61 and QGSJET-II.03 are also shown. Note that the 1σ band is narrow since the valence quark PDFs are expected to saturate and have weak dependence for high Q^2.

According to [22], RHIC data indicates that about 27% of the initial energy remains in the net-baryon after the collision. This result is also shown in the figure. It is apparent that EPOS, QGSJET-II and the present model show rather different trends. QGSJET-II is compatible with data but slightly above. At the same energies, the present model and EPOS are both somewhat below the measured value, but within 2σ. At higher energies, while in EPOS 1.61 the net-baryon is essentially zero, in the present model, and even more in QGSJET-II.03, a sizable amount of energy is still associated to the net-baryon. It should however be noted that high energy effects such as string percolation may change these predictions [25].

V. Conclusion

Making use of valence string formation mechanisms based on the standard PDFs with QCD evolution and string fragmentation via the Schwinger mechanism we built a simple but consistent model for net-baryon production in high energy hadron-hadron, hadron-nucleus and nucleus-nucleus. The obtained results, when compared to data and simulations, show that a good description of the main features of net-baryon data is achieved. In this simple model all the fundamental production mechanisms appear in a transparent way.

The two free parameters in our model, the effective Q^2 and

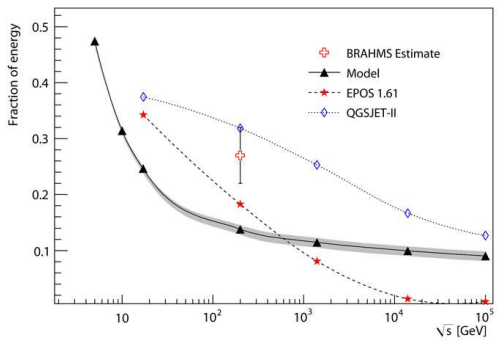

Fig. 10. Evolution of the fraction of energy carried by the net-baryon with $\sqrt{s}$. The prediction of the present model (with a shaded band corresponding to the 1σ variation of the fit parameters) is shown, together with the results obtained with EPOS and QGSJET-II. The data point corresponds to the RHIC estimate given in [22].

the number of participating nucleons, were fitted to the net-proton data at $\sqrt{s} \simeq 5$, 17 and 200 GeV. At $\sqrt{s} \simeq 5$ and 17, the values obtained for the number of participants are in agreement with what we would expect from the literature. At 200 GeV, present data cover only the mid-rapidity range, and the fit is too unconstrained to provide useful bounds on the parameters of the model. We want to stress the need for more net-baryon data at higher energies and higher rapidities. A relation between the effective Q^2 and the centre-of-mass energy was obtained using the (scarce) net-baryon data at different energies. This expression was extrapolated to higher energies in order to predict the fraction of initial energy carried away by the net-baryon. In this model a sizable amount of energy may be associated to the net-baryon even at high energies.

ACKNOWLEDGEMENTS

We thank K. Werner for kindly providing us the EPOS 1.61 code and for useful discussions and advice on its usage and results. We thank S. Ostapchenko for kindly providing us a QGSJET-II.03 standalone heavy-ion version and for useful discussions. We thank N. Armesto and S. Andringa for useful discussions. The presenter, R. Conceição, acknowledge the support of FCT, Fundação para a Ciência e a Tecnologia, Portugal.

REFERENCES

[1] J. Dias de Deus and J.G. Milhano, arXiv:0708.1717 [hep-ph].
[2] B.B. Back, Phys. Rev. C 72 (2005).
[3] N.N. Kalmykov, S.S. Ostapchenko, Yad. Fiz. 56 (1993) 105; Phys. At. Nucl. 56 N3 (1993) 346; N.N. Kalmykov, S.S. Ostapchenko, A.I. Pavlov, Izv. RAN Ser. Fiz. 58 (1994) N12 p.21; Bull. Russ. Acad. Science (Physics) 58 (1994) 1966; Nucl. Phys. B (Proc. Suppl.) 52 B (1997) 17.
[4] S.S. Ostapchenko, Nucl. Phys. B (Proc. Suppl.) 151 (2006) 143 and 147; Phys. Rev. D 74 (2006) 014026; private communications.
[5] K. Werner, F.M. Liu and T. Pierog, Phys. Rev. C 74 (2006) 044902; K. Werner, private communications.
[6] R.S. Fletcher, T.K. Gaisser, P. Lipari, T. Stanev, Phys. Rev. D 50 (1994) 5710; J. Engel, T.K. Gaisser, P. Lipari, T. Stanev, Phys. Rev. D 46 (1992) 5013; R. Engel, T.K. Gaisser, P. Lipari, T. Stanev, Proc. 26^{th} ICRC, Salt Lake City (USA), 1 (1999) 415.
[7] L. Van Hove, S. Pokorski, Nucl. Phys. B 86 (1975) 245; L. Van Hove, Acta Phys. Pol. B 7 (1976) 339.
[8] R.P. Feynman, Phys. Rev. Lett. 23 (1969).
[9] A. Capella, U. Sukhatme, C.-I. Tan, J. Tran Thanh Van, Phys.Rept. 236 (1994) 225-329.
[10] BRAHMS Collab., I.G. Bearden et. al., Phys. Rev. Lett. 93 (2004) 102301.
[11] Glauber, RJ. 1959. In Lectures in Theoretical Physics, ed. WE Brittin and LG Dunham, 1:315. New York: Interscience; M.L. Miller, K. Reygers, S.J. Sanders, P. Steinberg, nucl-ex/0701025.
[12] E802 Collab., L. Ahle et al., Phys. Rev. C 60 (1999) 064901; E877 Collab., J. Barette et al., Phys. Rev. C 62 (2000) 024901; E917 Collaboration, B.B. Back et al., Phys. Rev. C 66 (2002) 054901.
[13] NA49 Collab., H. Appelshauser et al., Phys. Rev. Lett. 82 (1999) 2471.
[14] C.E. Aguiar, R. Andrade, F. Grassi, Y. Hama, T. Kodama, T. Osada and O. Socolowski Jr., Brazilian Journal of Physics, Vol. 34, no. 1A (2004) 319.
[15] S.A. Bass, B. Muller and D.K. Srivastava, Phys. Rev. Lett. 91 (2003) 052302;
[16] J. Pumplin, D.R. Stump, J.Huston, H.L. Lai, P. Nadolsky, W.K. Tung, JHEP 0207 (2002) 012; D. Stump, J. Huston, J. Pumplin, W.K. Tung, H.L. Lai, S. Kuhlmann, J. Owens, JHEP 0310 (2003) 046; S. Kretzer, H.L. Lai, F. Olness, W.K. Tung, Phys. Rev. D 69(2004) 114005.
[17] D. Kharzeev, Phys. Lett. B 378 (1996) 238; A. Capella, B.Z. Kopeliovich, Phys. Lett. B 381 (1996) 325; S.E. Vance, M. Gyulassy, X.N. Wang, Phys. Lett. B 443 (1998) 45; S.E. Vance, M. Gyulassy, Phys. Rev. Lett. 83 (1999) 1735.
[18] G.H. Arakelian, A. Capella, A.B. Kaidalov, Yu.M. Shabelski, Eur. Phys. J. C 26 (2002) 81; F. Bopp, Yu.M. Shabelski, Eur. Phys. J. A 28 (2006) 237.
[19] B. Andersson, G. Gustafson, T. Sjöstrand, Nucl. Phys. B 197 (1982) 45; B. Andersson, G. Gustafson, T. Sjöstrand, Physica Scripta 32 (1985) 574; P. Edén, G. Gustafson, Z. Phys. C75 (1997) 41.
[20] K.J. Eskola, V.J. Kolhinen and C.A. Salgado, Eur. Phys. J. C. 9 (1999) 61; K.J. Eskola, V.J. Kolhinen and P.V. Ruuskanen, Nucl. Phys. B 535 (1998) 351.
[21] D. de Florian, R. Sassot, Phys. Rev. D 69 (2004) 074028.
[22] B.B. Back, nucl-ex/0508018.
[23] D. Kharzeev and M. Nardi, nucl-th/0012025.
[24] V.A. Abramovsky, E.V. Gedalin, E.G. Gurvich, O.V. Kancheli, Sov. J. Nucl. Phys. 53 (1991) 172-176; N.S. Amelin, N. Armesto, C. Pajares, D. Sousa, Eur. Phys. J. C 22 (2001) 149-163.
[25] J. Alvarez-Muñiz, P. Brogueira, R. Conceição, J. Dias de Deus, M. C. Espírito Santo and M. Pimenta, Astropart. Phys. 27 (2007) 271; J. Dias de Deus, M. C. Espírito Santo, M. Pimenta and C. Pajares, Phys. Rev. Lett. 96 (2006) 162001.